Influence of Segmental Swelling Ratio of a Symmetric Block Copolymer on the Morphology of Melt-Mixed Immiscible Polymer Blends

Jong Ryang Kim, Alex M. Jamieson,* Steven D. Hudson, Ica Manas-Zloczower, and Hatsuo Ishida

Department of Macromolecular Science, Case Western Reserve University, Cleveland, Ohio 44106

Received February 8, 1999; Revised Manuscript Received May 12, 1999

ABSTRACT: We investigate droplet breakup and coalescence under shear flow for an immiscible polymer blend system in which styrene−acrylonitrile random copolymer and poly(cyclohexyl methacrylate) are the blend components, and a symmetric poly(styrene-*b*-methyl methacrylate) block copolymer (bcp) is utilized as a compatibilizer. The influence on the blend morphology of the ratio (S_r) between the swelling power at the interface of the bcp segment outside the droplet versus that inside the droplet is studied. We find that the balance of swelling between external and internal segments has an important influence on the ultimate blend morphology. Four zones of morphological behaviors are observed: $S_r < 0.4$, internal emulsification failure; $1 > S_r > 0.4$, unstable emulsification; $2.5 > S_r > 1$, stable emulsification; $S_r > 2.5$, external emulsification failure.

Introduction

It is well-known that a block copolymer (bcp) is effective as an emulsifier for immiscible polymer blends, and the effect of a bcp in producing a more finely divided morphology has been established experimentally.[1−3] The size of droplets in immiscible polymer blends is known to be governed by the balance between the viscous deformation force on the droplets and the interfacial energy in systems exhibiting a Newtonian flow behavior.[4] Analysis of this force balance leads to the following relationship:[4,5]

$$D = \frac{4\Gamma(\eta_r + 1)}{\dot{\gamma}\eta_m\left(\frac{19}{4}\eta_r + 4\right)}, \quad \eta_r \le 1 \tag{1}$$

where D is the maximum stable size of the droplet, Γ is the interfacial tension, η_r is the relative viscosity which is the ratio of the viscosity of droplet (η_d) to that of matrix (η_m), and $\dot{\gamma}$ is the shear rate.

The emulsification of immiscible blends by a block copolymer has been interpreted as the result of the ability of bcp to decrease the interfacial tension by being located at the interface.[6,7] Recently, however, this role has been reevaluated. The bcp may not only decrease the interfacial tension[6] but also inhibit the coalescence of droplets by inhibiting film drainage, e.g., by immobilizing the interface[3] or by decreasing the collision frequency due to an effect of the block copolymer on the flow within and between droplets during close encounters.[8]

There have been few systematic studies of the role of the interactions between bcp segments and the corresponding blend components on droplet breakup and coalescence. Recently, we demonstrated that an exothermic interaction between a bcp segment and a blend component can influence the coalescence rate markedly.[9] On the basis of our observations, we proposed that the balance of segmental swelling factors of the bcp at the interface by the homopolymers is important to determine the ultimate blend morphology. Here, the segmental swelling power (S_{ij}) of homopolymer i in copolymer segment j can be expressed theoretically by the following equation:[10,11]

$$S_{ij} = N_j/P_i - 2\chi_{ij}N_j \tag{2}$$

where N_j is the degree of polymerization of segment j of the block copolymer and P_i is that of the blend component i and χ_{ij} is the Flory−Huggins parameter characterizing the interaction between the bcp segment and the compatible blend component. Note that eq 2 neglects the effect of interactions between the incompatible block segments and polymers across the interface. This approximation is expected to be valid for the wet brush limit, where the block segments are highly swollen, $S_{ij} \gg 1$. Also, note this expression does not apply when S_{ij}, as defined, is less than 1.

In the present study, we investigate further the influence of the balance of swelling between the two segments of a diblock copolymer on the breakup and coalescence of immiscible polymer blends. Each segment of the diblock copolymer has an exothermic interaction with the blend components. The blend system has poly(cyclohexyl methacrylate) (PCHMA) and a random styrene−acrylonitrile copolymer (SAN) as the major and minor blend components. Poly(styrene-*b*-methyl methacrylate) diblock copolymer (bcp) is utilized as an emulsifier where the PS block is miscible with PCHMA and the PMMA block is miscible with SAN. By inverting the blend composition, we can carry out a study where the ratio of swelling factors between discrete and continuous phases is likewise inverted.

Experimental Section

The blend components used in this study are a 299K PMMA-*b*-PS block copolymer (155K:144K; $M_w/M_n = 1.12$), from Polymer Source Inc., PCHMA ($M_n = 38.5$K; $M_w/M_n = 3.47$) from Scientific Polymer Products Inc., and styrene−acrylonitrile copolymers (SAN) with 26% and 33% acrylonitrile content (respectively $M_w = 153$K and 130K; $M_w/M_n = 2.23$ and 1.95) supplied by Mitsui Toatsu Chemical Inc. The weight ratio of major and minor component is 4:1, and 5% of bcp was added to the blend system without changing the ratio of major and minor component.

10.1021/ma990177h CCC: $18.00
Published on Web 06/17/1999

For melt blending in the rheometer, crude mixtures were first prepared by dry mixing the blend components in powder form. In preparing blends containing the bcp, the bcp and the minor phase constituent were first dissolved in MEK solvent and coprecipitated, and the precipitates were dried in a vacuum oven for 24 h at room temperature. This material in powder form was then dry mixed with the major phase. This procedure facilitates migration of the bcp to the phase boundary. The dry mixed powders were molded to form disks at 200 °C under vacuum in a Carver Lab Press compression molding machine. Hereafter, the blend systems are expressed as component A/component B/bcp where components A and B are major and minor components, respectively.

Disk samples, prepared as described above, were sheared in parallel plate geometry, with diameter 7.9 mm and gap 0.5 mm at 200 °C, using the Rheometrics RMS 800 rheometer. Shearing was first performed at a higher shear rate of 50 s^{-1} for blends with SAN as the major phase and 20 s^{-1} for blends with PCHMA as the major phase, to produce breakup of large droplets of the minor phase. After shearing at 50 or 20 s^{-1} for 20 min, a low shear rate of 1 s^{-1} was applied suddenly for a specified time period, to allow shear-induced coalescence of the small droplets. After shearing, the samples were allowed 1 min of equilibration time followed by rapid cooling with liquid nitrogen. The time required for the temperature to fall from the processing condition at 200 °C to the point at which the glass transition occurs (~100 °C) was 30 s.

A JEOL 100 CX TEM with an acceleration voltage of 100 kV was used to investigate the morphologies of processed blends. TEM observations were made in the maximum shear region of the sample. The perimeter areas of the melt blended disk specimens were sectioned into ultrathin films of 50−80 nm thickness using a diamond knife and a RMC Inc. MT-7000 ultramicrotome machine. Velocity and velocity gradient directions were parallel to the section plane. Sectioned films were exposed to RuO_4 vapor for 14 min in an enclosed chamber containing 0.25% aqueous solution of RuO_4. The PS segment of the bcp and the SANs are stained with RuO_4 such that the PS segment is seen as the darkest, and the SAN phase is light gray. PCHMA is unstained by RuO_4. Therefore, microdomains of the bcp at the droplet interface or as micelles can be detected.

NIH image software[12] was used to calculate the statistical sizes of the droplets from the TEM micrographs of the blends. Number-average droplet diameters were calculated. The number of droplets in the calculation was at least 100, except in the case of 20 min of shearing time at 1 s^{-1} for the systems without bcp in which at least 50 droplets were used to calculate the average droplet sizes. The accuracy of binary thresholded images was checked by comparing with the original images. For nonspherical droplets, diameters were estimated from the areas determined by the NIH software, using area $= \pi(D/2)^2$. The measured droplet sizes were converted to the weight-average droplet size which is defined as

$$D_w = \Sigma(nD^4)/\Sigma(nD^3) \quad (3)$$

The diameters of some of the droplets viewed in a microtomed section will be underestimated, when the section plane does not intersect the droplet center. On the other hand, small particles can be undercounted since the probability of sectioning them is smaller. These potential errors compensate each other, such that the error in the average droplet size is estimated to be less than 10%. Hence, the experimental trends are unaffected by these errors.[1] Therefore, we use the droplet size measured by the software directly without correction.

Results and Discussion

The swelling powers (S) for the four different blend systems were calculated using eq 2. The calculated swelling powers for the outside and inside bcp segments at the droplet interface (S_{out} and S_{in}) and the ratio S_{out}/S_{in} are listed in Table 1. In calculating the swelling power for polydisperse materials based on the Flory−Huggins theory, it is appropriate to use the number-average molecular weight M_n. Previous analysis of solvent-cast blends consisting of mixtures of monodisperse PS and PMMA with PS-*b*-PMMA bcp confirms that M_n is more applicable when modeling blend morphology.[13] By simple inversion of the major and minor components (PCHMA and SANs), it is evidently possible to design different combinations of S_{out}, S_{in}, and their ratios without significantly changing the interfacial tension.

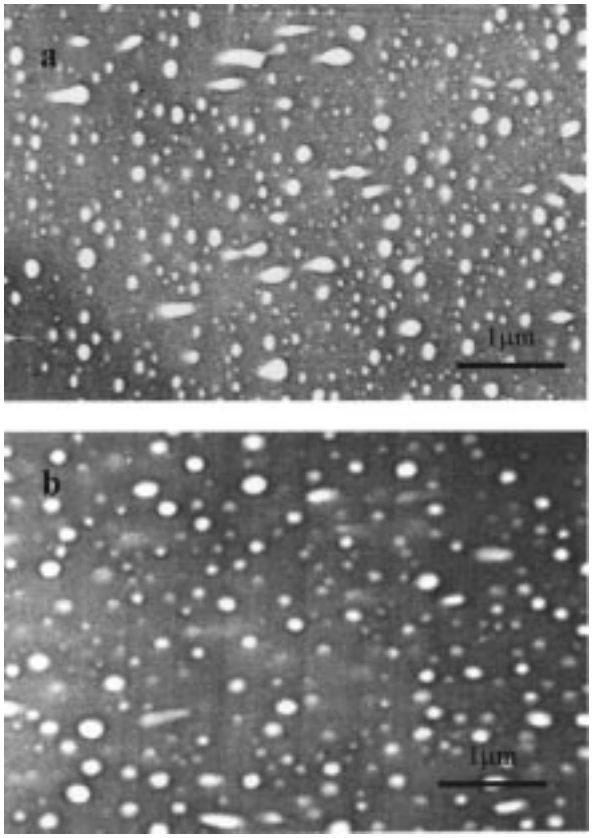

Figure 1. TEM micrograms of SAN26/PCHMA/bcp sheared at (a) 50 s^{-1} for 20 min and (b) 1 s^{-1} for 20 min after shearing at 50 s^{-1} for 20 min.

Table 1. Segmental Swelling Power and Swelling Ratio in the Blend Systems Studied

major component/minor component/bcp	S_{out}	S_{in}	S_{out}/S_{in}
SAN26/PCHMA/bcp	30.8	15.2	2.0
SAN33/PCHMA/bcp	3.5	15.2	0.23
PCHMA/SAN26/bcp	15.2	30.8	0.49
PCHMA/SAN33/bcp	15.2	3.5	4.3

As previously demonstrated in our earlier study,[9] in the SAN26/PCHMA/bcp system, when SAN is the matrix component and the swelling ratio S_{out}/S_{in} is 2.0, the minor component, PCHMA, is dispersed into small droplets after breakup at high shear rates, and these small droplets are stabilized so that no coalescence is observed (Figure 1a,b). In this case, the swelling ratio is larger than 1 so that the spontaneous curvature of the interface has the same direction as that of the droplet shape (convex toward the matrix). Thus, the droplets become thoroughly emulsified. Indeed, with 5% bcp, no coalescence occurs. The droplet size may be close to the equilibrium size as suggested by the observation that the morphology of the solvent cast blend shows

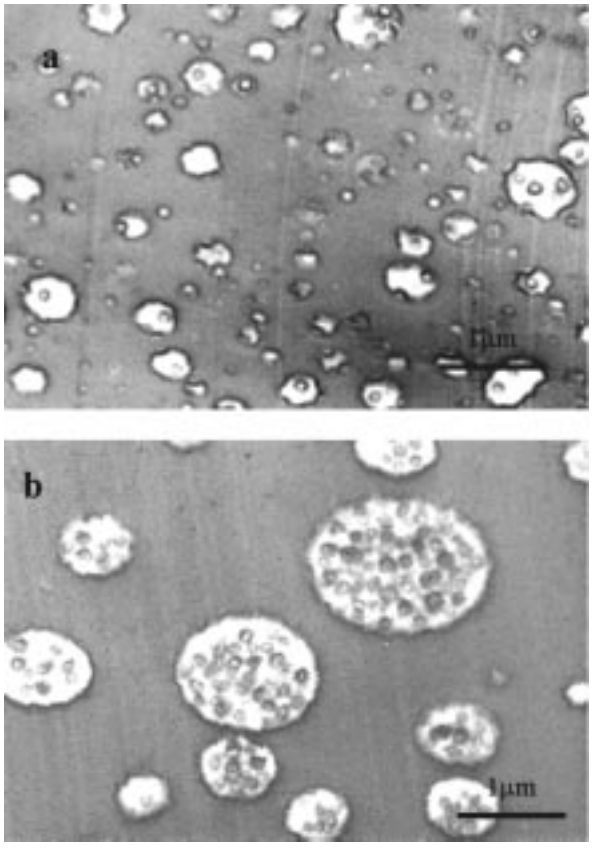

Figure 2. TEM micrograms of SAN33/PCHMA/bcp sheared at (a) 50 s^{-1} for 20 min and (b) 1 s^{-1} for 20 min after shearing at 50 s^{-1} for 20 min.

spherical droplets of similar sizes.[9] Adedeji et al.[14] have previously shown that the morphology of dispersed droplets in solvent cast A/B/bcp blends with $S_{out}/S_{in} \geq 1$ is spherical.

In contrast, in the SAN33/PCHMA/bcp system, which has a swelling ratio of 0.23, although small droplets are well distributed at high shear (Figure 2a), they do coalesce into larger droplets at lower shear rate (Figure 2b). However, coalescence occurs at a slower rate in comparison with the uncompatibilized blend.[9] In this system, the larger droplets contain excess bcp in the form of micelles within their interiors as clearly evident in Figure 2b. Kim et al.[9] have presented evidence that, for this blend, the equilibrium blend morphology consists of vesicles of the minor component. However, in melt blending, this morphology is not obtained.

In describing our observations on the PCHMA/SAN33/bcp and PCHMA/SAN26/bcp blends, we first realize that, by inverting the compositions, we change the viscosity of the matrix (η_m) and dispersed phase (η_d), as well as the swelling factor ratio S_{out}/S_{in}. As indicated by the Taylor equation (eq 1), the viscosity parameters η_m and $\eta_r = \eta_d/\eta_m$ can influence the droplet size of the dispersed phase. In the absence of bcp, both PCHMA/SAN26 and PCHMA/SAN33 show droplet coalescence when subjected to an initial shear of 20 s^{-1} for 20 min, followed by 20 min at 1 s^{-1} (Figure 3). Most striking is the disappearance of small droplets during the low-shear period.

Table 2 compares the measured number-average droplet sizes in the absence of bcp versus those predicted by the Taylor equation using the system parameters also listed in Table 2. While qualitatively consistent with the theory, the predicted values are substantially smaller than measured, as was observed earlier for the SAN33/PCHMA and SAN26/PCHMA blends.[9] The discrepancy arises, perhaps, because of a large influence of polymer elasticity on droplet breakup. Mighri et al.[15] recently investigated the influence of elasticity ratio (k_r) on breakup of droplets in simple shear. Here, the elasticity ratio is the ratio of the Maxwell relaxation time of the droplet (λ_d) to that of the matrix (λ_m) where the Maxwell relaxation time is defined as $\lambda = N_1/2\eta\dot{\gamma}^2$ and N_1 is the first normal stress difference. Mighri et al.[15] found that the droplet size increases with increase of k_r when $k_r > 0.37$ and levels off when $k_r > 4$. An empirical correction was performed to our calculated droplet sizes based on the experimental results of Mighri et al., using the measured first normal stresses for each of the blend components (Table 2). The corrected droplet sizes, D_{corr}, are listed in Table 2. By incorporating the influence of elasticity, the calculated and measured droplet sizes become more self-consistent, although substantial discrepancies still remain. In any event, the viscosity parameters η_m and η_r are very similar for both PCHMA/SAN33 and PCHMA/SAN26 blends, and hence, as before,[9] we can expect to isolate the influence of bcp swelling ratio on blend morphology.

On addition of 5% bcp, as shown in Figure 4a,b, for PCHMA/SAN26/bcp, and Figure 5a,b, for PCHMA/SAN33/bcp, coalescence still occurs, but in each case, the average droplet sizes, after high-shear followed by low-shear processing, are substantially smaller than in the nonemulsified blend.

In the PCHMA/SAN26/bcp system, $S_{out}/S_{in} = 0.49$, and consistent with our observations on the SAN33/PCHMA/bcp blend ($S_{out}/S_{in} = 0.23$), the droplets exhibit coalescence. When the swelling power ratio is less than 1, i.e., $S_{out} < S_{in}$, the spontaneous curvature (concave toward the exterior of the droplet) is opposite to that produced by shear; hence, the droplet sizes after high shear are not stable. A simple physical argument indicates that, in this situation, the film between two droplets in a close encounter will rupture easily. During the film drainage as the droplets approach each other, the curvature of the film interface approaches zero. If the spontaneous curvature is convex toward the matrix, the tendency is for the droplets to tumble past each other so that no coalescence occurs. On the other hand, when the spontaneous curvature is concave toward the matrix, encapsulation of the film between the droplets will lead to film rupture and coalescence with a small energy cost. Thus, the same bcp has a quite different effect on droplet coalescence in the SAN26/PCHMA/bcp compared to the PCHMA/SAN26/bcp system, where the matrix and droplet phase are inverted (compare Figure 1 with Figure 4). The distinct coalescence behavior arises because of the difference in the swelling power ratio (2.0 versus 0.49). We further note that, in the SAN33/PCHMA/bcp blend, for which the swelling power imbalance is smallest, the coalescence rate is faster, and micelles appear within the coalesced droplets (Figure 2).

In the PCHMA/SAN33/bcp system, which has a swelling ratio of $S_{out}/S_{in} = 4.3$, droplet coalescence is also observed, and the morphology shows very small micelles in the matrix coexisting with larger coalesced droplets (Figure 5a,b). This discrete bimodal size distribution is characteristic of emulsification failure, which has been described theoretically[6,16] and experi-

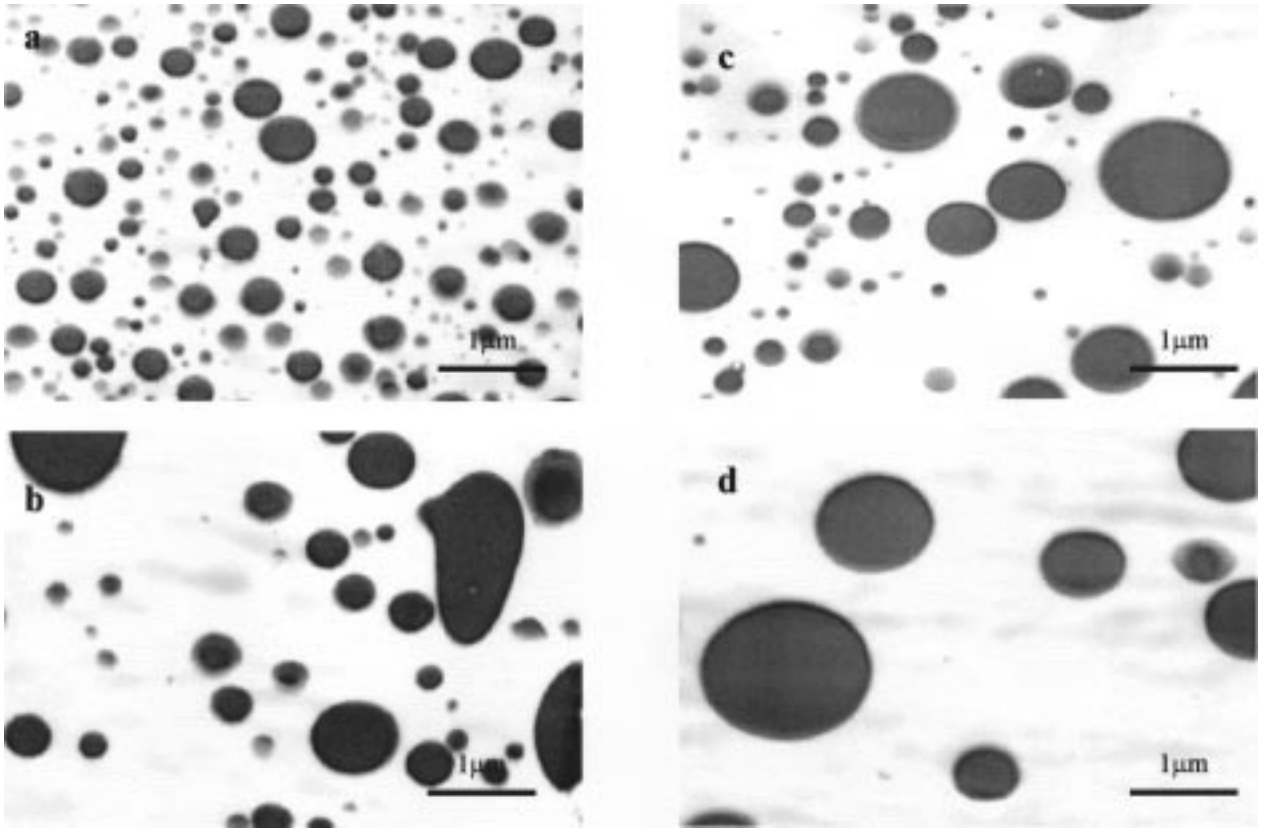

Figure 3. TEM micrograms of uncompatibilized blend systems (a) PCHMA/SAN26 sheared at 20 s^{-1} for 20 min, (b) PCHMA/SAN26 sheared at 1 s^{-1} after shearing at 20 s^{-1} for 20 min, (c) PCHMA/SAN33 sheared at 20 s^{-1} for 20 min, and (d) PCHMA/SAN33 sheared at 1 s^{-1} after shearing at 20 s^{-1} for 20 min.

Table 2. Calculated Values of Flory−Huggins Parameter (χ), Interfacial Tension (Γ), and Droplet Size (D) for the Uncompatibilized Blends

	PCHMA/SAN26		PCHMA/SAN33	
$\dot{\gamma}$ (s^{-1})	20	1	20	1
η_m (Pa·s)	4260	12900	4260	12900
η_d (Pa·s)	2080	7210	1920	6130
η_r	0.49	0.56	0.45	0.48
χ	0.0236	0.0236	0.0473	0.0473
Γ (mN/m)	1.73	1.73	2.44	2.44
D_{Taylor} (μm)	0.019	0.125	0.027	0.178
N_1 (kN/m^2)	470/250	17/8.3	470/150	17/4.8
D_{corr} (μm)	0.05	0.29	0.06	0.37
$D_{w,exp}$ (μm)	0.35	0.93	0.76	1.2

mentally[17] in solvent-cast blend systems. Emulsification failure occurs when the interfacial tension is finite at the point that the interface is saturated with copolymer, and excess copolymer exists in micelles within the phase in which it is more soluble.[6,16] (Note that micelles may be swollen with homopolymer.) The term failure is used, because only some of the copolymer is at the macrophase interface, and the rest of the copolymer is ineffective in reducing the droplet size. When the swelling ratio S_{out}/S_{in} is large, the spontaneous curvature is very pronounced, and micelles are favored in the continuous phase. We term this situation external emulsification failure. In contrast, for the blend with the inverse composition, SAN33/PCHMA/bcp, the swelling ratio ($S_{out}/S_{in} = 0.23$) is very low, and micelles form inside the droplets (Figure 2b). The micelles form inside the droplets because of the stronger affinity of the PS segment for the minor PCHMA phase. We term this situation internal emulsification failure. Note that the microscopic sizes of the micelles produced in both external and internal emulsification failure are similar (Figures 2b and 5b).

The theoretical analyses of Leibler[6] and Wang and Safran[16] consider that the macrodomain interface is planar. While the phase boundaries in our experiments are clearly not planar, their curvature is approximately an order of magnitude less than that of the micelles. Therefore, the equilibrium condition between adsorbed bcp and micelles is expected to be nearly equivalent. The theoretical analyses considered asymmetry in the molecular weight of the two brushes. Leibler[6] found in the dry brush limit (in which the homopolymer swelling power is irrelevant) that emulsification failure occurs when the ratio of the block molecular weights is less than 0.45 or greater than 2.2. According to calculations that we will report elsewhere, asymmetry in the swelling power of the block copolymer brushes by the respective homopolymers is expected to have a similar effect.

Our observations suggest that, as for solvent-cast blends,[17] for melt mixed immiscible blends, a window exists in the emulsification effectiveness of a bcp. This window depends on the balance at the blend interface between the bcp segmental swelling ratios (Figure 6). When the swelling ratio is close to or slightly larger than 1, the bcp is effective in producing well-distributed droplets of small size. If the ratio is much larger than 1, we expect external emulsification failure due to the high interfacial curvature (convex toward the major component). The boundary between good emulsification and emulsification failure depends on the concentration of bcp and the degree of swelling imbalance. When the swelling ratio is slightly smaller than 1, there is slow coalescence possibly due to the ease of rupture of the

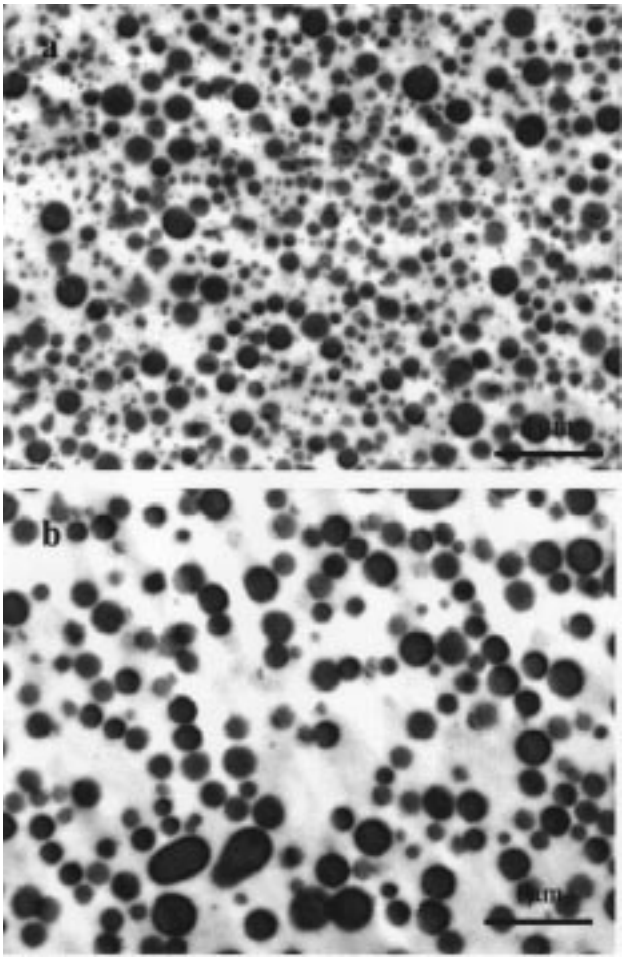

Figure 4. TEM micrograms of PCHMA/SAN26/bcp sheared at (a) 20 s^{-1} for 20 min and (b) 1 s^{-1} for 20 min after sheared at 20 s^{-1} for 20 min.

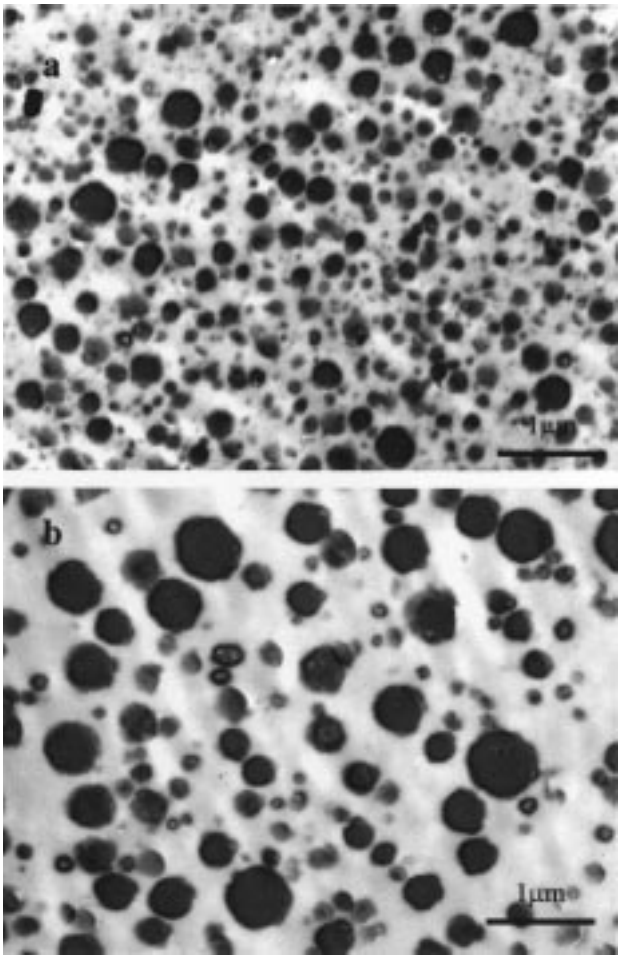

Figure 5. TEM micrograms of PCHMA/SAN33/bcp sheared at (a) 20 s^{-1} for 20 min and (b) 1 s^{-1} for 20 min after sheared at 20 s^{-1} for 20 min.

draining film between droplets during close encounters. If the swelling ratio is much smaller than 1, more rapid coalescence is observed because of internal emulsification failure due to the high convex curvature toward the minor component. In Figure 6, we located the boundaries between stable emulsification versus external and internal emulsification failure at $S_{out}/S_{in} < 2.5$ and $S_{out}/S_{in} > 0.4$, respectively. These values are nearly consistent with Leibler's theoretical analysis,[6] discussed above. However, we recognize that our present conclusions are based on only four blend systems, and a wider range of blends must be investigated to clarify the details of Figure 6.

The interfacial area occupied by a bcp molecule, Σ_w, was calculated on the basis of the measured weight-average droplet size, the volume fraction of the minor component, the concentration of added bcp, and assuming that all bcp is at the interface (Table 3). The values are significantly larger than that of the pure bcp ($\Sigma =$ 12 nm^2) calculated on the basis of the lamellar morphology. This means that the bcp segments in the blend systems are considerably swollen by the blend components. For instance, in the case of SAN26/PCHMA/bcp, where high shear produces a finely divided morphology comparable to that of the solvent-cast (near-equilibrium) blend, Σ_w is almost 6−7 times larger than that of pure bcp.

The ratios Σ_w/Σ_a are also shown in Table 3, where Σ_a is the interfacial area occupied by one bcp molecule

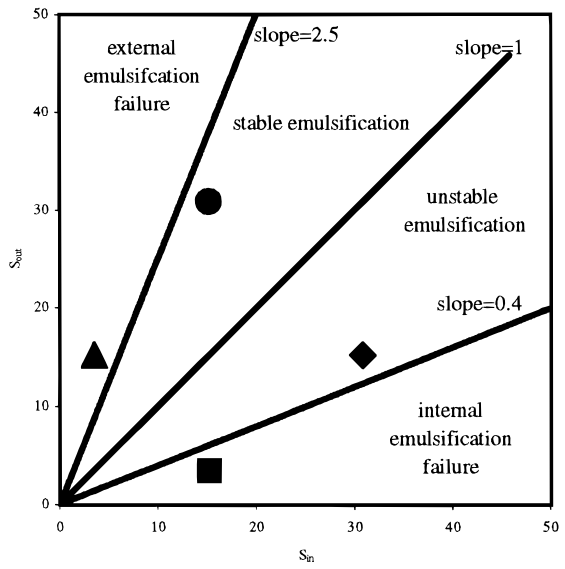

Figure 6. Coalescence diagram based on the swelling power balance.

calculated from the areal-average droplet size: $D_a = \Sigma n_i D_i^3/\Sigma n_i D_i^2$. The values of Σ_w/Σ_a are sensitive to the size polydispersity of droplets, with lower values of Σ_w/Σ_a implying a broader size polydispersity. We compare the values at low shear rates where coalescence is facile. The value for the PCHMA/SAN33/bcp blend system (~0.59) is distinctly smaller than those of the other

Table 3. Interfacial Area Occupied by One bcp Molecule for the Compatibilized Blends

	shear rate (s^{-1})	D_w (μm)	Σ_w (nm^2)	Σ_w/Σ_a[a]
SAN33/PCHMA/bcp	50	0.56	20	0.52
	1	0.96	12[b]	0.71
SAN26/PCHMA/bcp	50	0.15	75	0.73
	1	0.14	81	0.71
PCHMA/SAN33/bcp	20	0.35	32	0.60
	1	0.55	21	0.58
PCHMA/SAN26/bcp	20	0.37	31	0.57
	1	0.45	25	0.87

[a] Σ_a is the interfacial area calculated from the areal average diameter. [b] This value is inaccurate since the internal micelles were not included in evaluating the average droplet size.

blend systems (0.7−0.8). This is another manifestation of emulsification failure, which leads to a broad size distribution due to the coexistence of small and larger droplets.

We note that it is important to remember that droplet sizes in these melt blended systems are also influenced by the shear history and hence by the viscosity and elasticity of the blend components (see Table 2). However, in the present study, we have maintained a relatively uniform processing history in order to isolate the influence of segmental swelling of the bcp on droplet breakup and coalescence. Finally, we point out that in all of the blend systems we have studied to date, the individual segmental swelling powers S_{out} and S_{in} are substantially larger than unity, i.e., our observations and conclusions apply under "wet brush" conditions. The factors that affect coalescence in the "dry brush" limit ($S_{ij} \sim 1.0$) need further investigation.

Conclusions

The influence of the balance of swelling between the exterior and interior segments of a symmetric bcp at the interface on droplet breakup and coalescence has been studied. At intermediate values of the swelling ratio, $1.0 < S_{out}/S_{in} < 2.5$, the droplet sizes of the minor phase reached under high shear are stabilized, and no coalescence is observed at low shear. However, when the swelling ratio is slightly smaller than 1 ($0.4 < S_{out}/S_{in}$), slow coalescence of droplets is observed. If $S_{out} \gg S_{in}$, external emulsification failure occurs, and at low shear, equilibrium droplets coexist with larger coalesced droplets. When $S_{out} \ll S_{in}$, internal emulsification failure occurs, and at low shear, coalescence occurs to form large droplets containing entrapped bcp micelles.

Acknowledgment. The financial support from Edison Polymer Innovation Corporation, the General Electric Company, and NSF Grant CTS-9731502 is gratefully acknowledged.

References and Notes

(1) Sundararaj, U.; Macosko, C. W. *Macromolecules* **1995**, *28*, 2647.
(2) Fayt, R.; Jerome, R.; Teyssie, Ph. *J. Polym. Sci., Phys. Ed.* **1982**, *20*, 2209.
(3) Fayt, R.; Jerome, R.; Teyssie, Ph. *Makromol. Chem.* **1986**, *187*, 837.
(4) Taylor, G. I. *Proc. R. Soc. London* **1934**, *A146*, 501.
(5) Grace, H. P. *Chem. Eng. Commun.* **1982**, *14*, 225.
(6) Leibler, L. *Macromol. Symp.* **1988**, *16*, 1.
(7) Noolandi, J.; Hong, K. M. *Macromolecules* **1982**, *15*, 482.
(8) Milner, S. T.; Xi, H. *J. Rheol.* **1996**, *40*, 663.
(9) Kim, J. R.; Jamieson, A. M.; Hudson, S. D.; Manas-Zloczower, I.; Ishida, H. *Macromolecules* **1998**, *31*, 5383.
(10) Adedeji, A.; Hudson, S. D.; Jamieson, A. M. *Polymer* **1997**, *38*, 737.
(11) Braun, H.; Rudolf, B.; Cantow, H. J. *Polym. Bull.* **1994**, *32*, 241.
(12) NIH image software is available on the Internet, http://rsb.info.nih.gov/nih-image/.
(13) Kim, J. R. Unpublished results, 1998.
(14) Adedeji, A.; Jamieson, A. M.; Hudson, S. D. *Macromol. Chem. Phys.* **1996**, *197*, 2521.
(15) Mighri, F.; Carreau, P. J.; Ajji, A. *J. Rheol.* **1998**, *42*, 1447.
(16) Wang, Z. G.; Safran, S. A. *J. Phys. (Paris)* **1990**, *51*, 185.
(17) Adedeji, A.; Hudson, S. D.; Jamieson, A. M. *Macromolecules* **1996**, *29*, 2449.

MA990177H